

Fig. 1

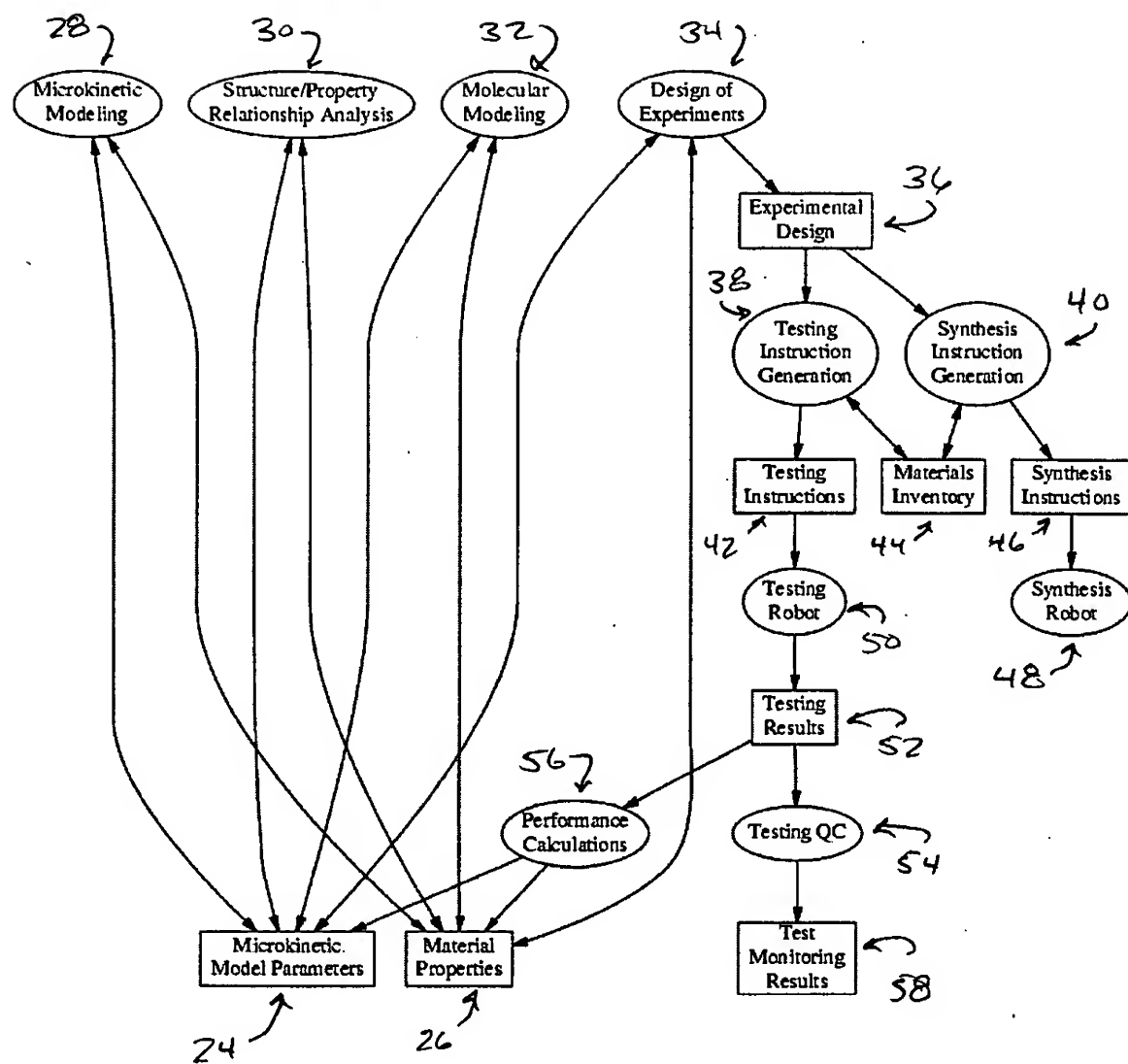


Fig. 2.

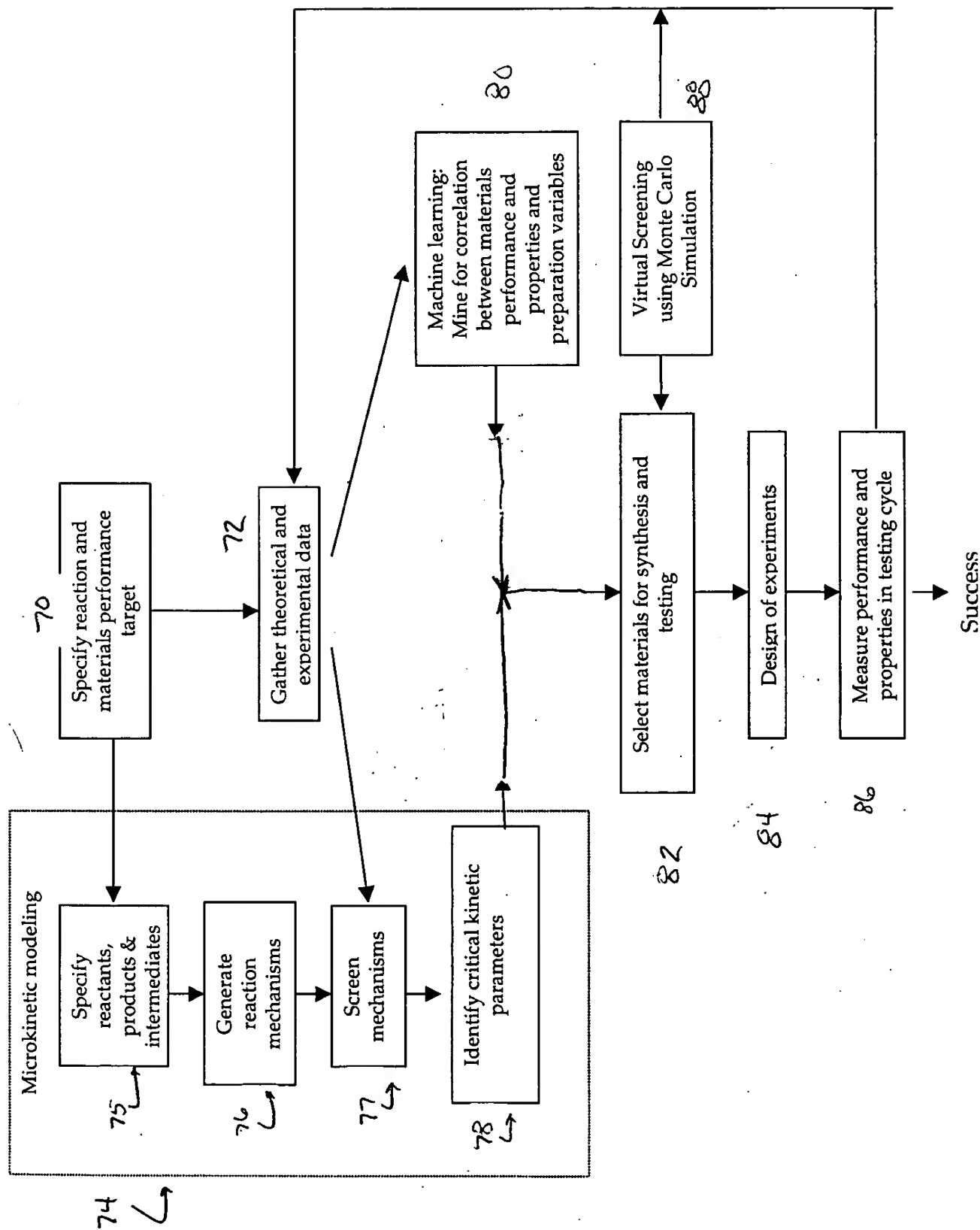
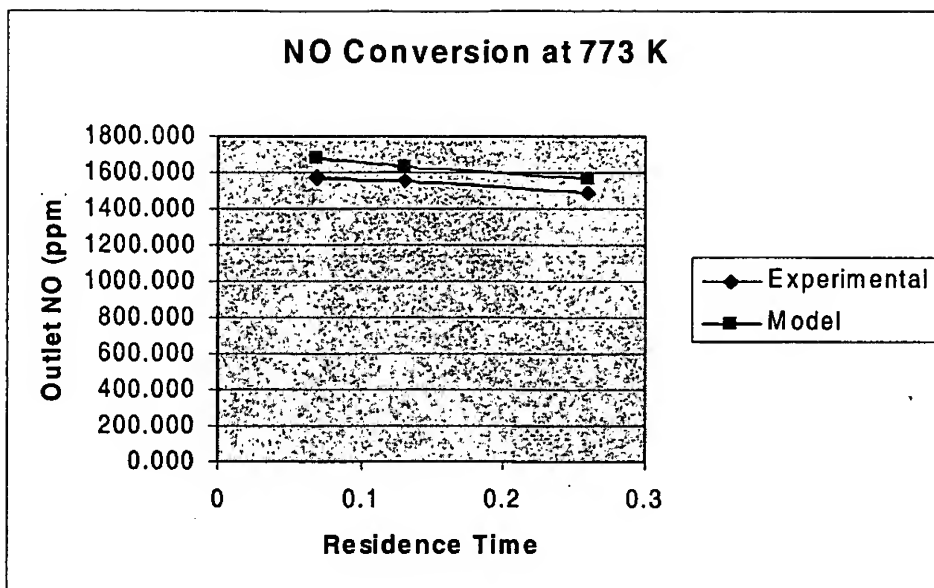
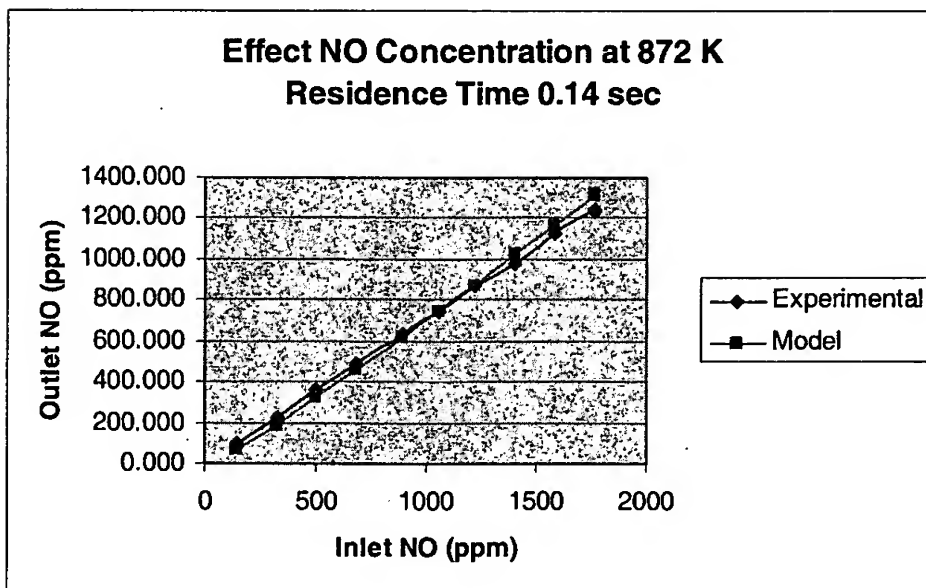


Fig. 3a



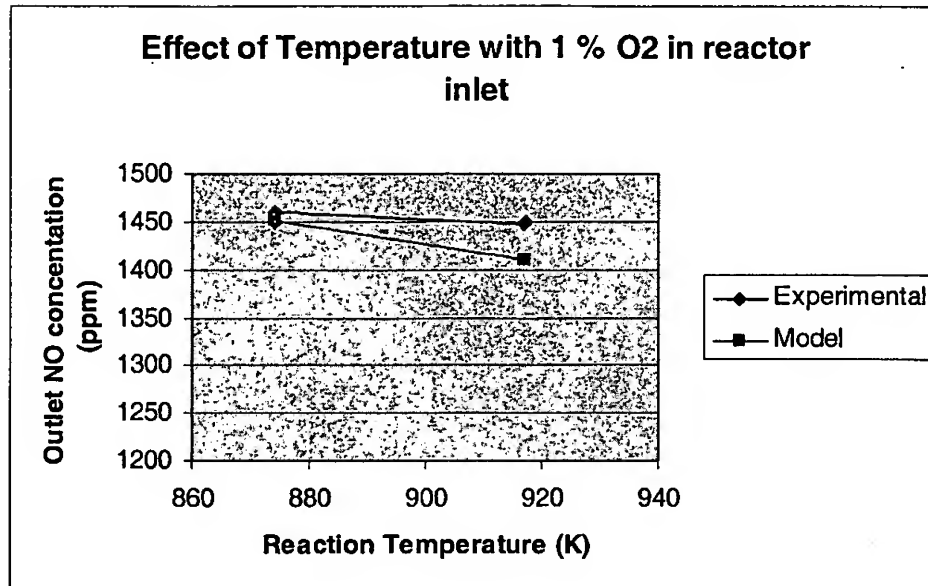
Inlet NO Conc. = 1760 ppm

Fig. 4a



Reaction is first order in NO

Fig. 4b

**Fig. 4c**

205020-1423001

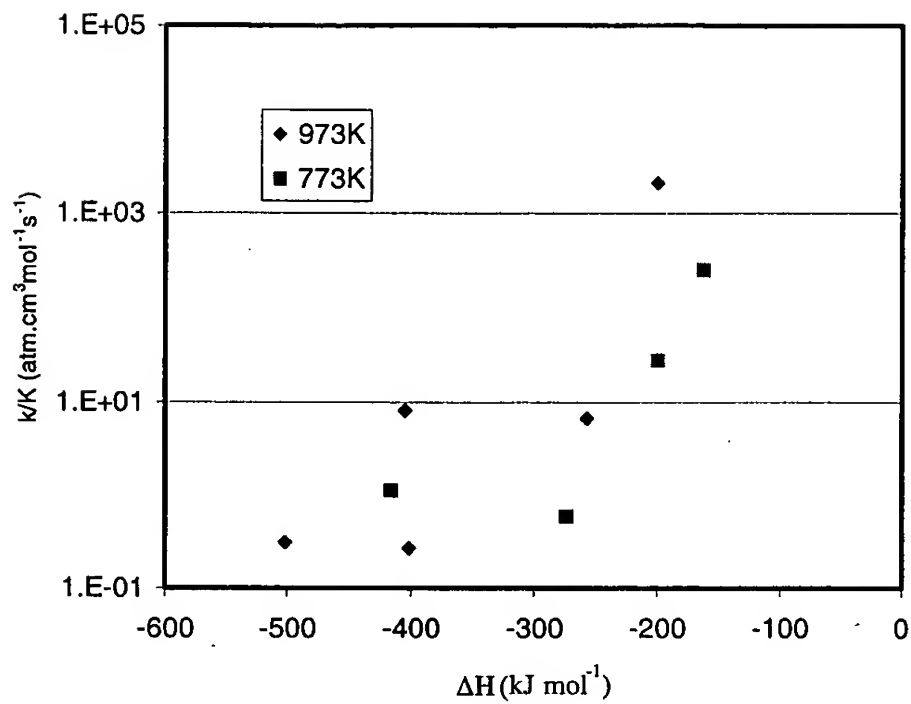
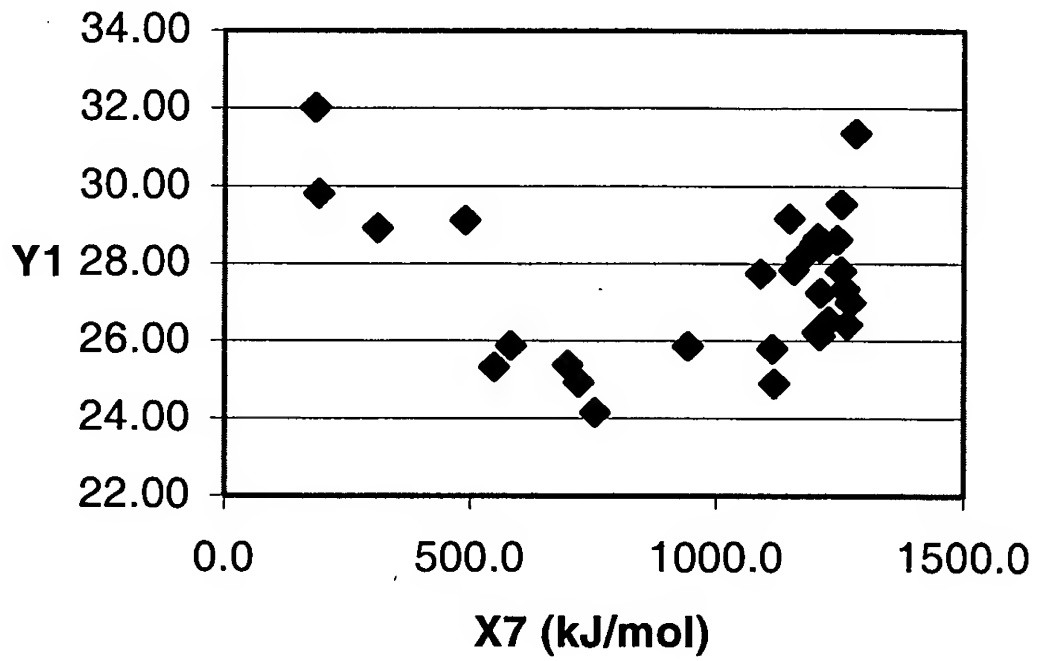


Fig. 5

FIG. 6

X1	X2	X3	X4	X5	X6	X7	X8	X9	X10	X11	X12	X13	X14	X15	X16	X17	X18	X19	X20	Y1	Y2
12	MgO	IIA	2800	38	35	1204.5	1.72	1.36	13.10	1.31	7.646	0.2260	1.560	10.60	1.736	1.756	1.662	0.110	cubic	26.24	37
13	Al ₂ O ₃	IIIA	2046.7	45	43	1117.0	1.82	1.18	16.50	1.61	5.986	0.3770	2.370	6.80	1.643	3.678	1.191	0.137	hexagonal	24.90	38
20	CaO	IIA	2587	30	34	1271.0	2.23	1.74	40.00	1.00	6.113	0.2980	2.000	22.80	1.837	2.886	2.416	0.088	cubic	27.01	28
21	SiO ₂	IIIB	2405	43	46	1147.2	2.09	1.44	315.00	1.36	6.540	0.0177	0.158	17.80	1.99	7.020	2.149	0.064	cubic	29.17	31
22	TiO ₂	IVB	1855	35	39	941.6	2.00	1.32	153.00	1.54	6.820	0.0234	0.219	14.60	2.616	4.931		0.021	Rutile	25.86	19
24	Cr ₂ O ₃	VIB	2300	38	40	753.6	1.85	1.18	180.00	1.66	6.766	0.0774	0.937	11.60	2.5	7.352	2.251	0.026	hexagonal	24.16	23
26	Fe ₂ O ₃	VIII	1562	27	22	548.5	1.72	1.17		1.83	7.870	0.0993	0.802	8.40	2.95	8.685	2.695	0.013	hexagonal	25.31	16
28	NiO	VIII	1957	45	39.5	489.0	1.62	1.15		1.91	7.635	0.1430	0.907	6.80	2.37	2.407		0.032	cubic	29.12	30
29	CuO	IB	1336	22	24	310.7	1.57	1.17	-5.46	1.90	7.726	0.5960	4.010	6.10	2.84	3.455		0.015		28.91	9
30	ZnO	IIIB	1975	36	42	696.7	1.53	1.25	-11.40	1.65	9.394	0.1660	1.160	7.10	2.004	2.882	2.382	0.062	hexagonal	25.38	41
31	Ga ₂ O ₃	IIIA	1740	40.5	40.5	720.1	1.81	1.26	-21.60	1.81	5.999	0.0678	0.406	8.12	1.935	5.506		0.071	hexagonal	24.93	29
38	SrO	IIA	2430	15	23	1282.8	2.45	1.91	92.00	0.95	5.995	0.0762	0.353	27.60	1.87	3.966	3.106	0.082	cubic	31.37	15
39	Y ₂ O ₃	IIIB	2376	18.5	27.5	1172.3	2.27	1.62	187.70	1.22	6.380	0.0166	0.172	22.70	1.91	8.662	2.521	0.075	cubic	28.14	24
45	Rh ₂ O ₃	VIII	1115	10	34	190.6	1.83	1.25	111.00	2.28	7.460	0.2110	1.500	8.60					rhombic	29.81	14
50	SnO ₂	IVA	1625	27	32	581.1	1.72	1.41	-37.00	1.96	7.344	0.0917	0.666	7.70	1.997	4.284		0.063	tetragonal	25.89	19
57	La ₂ O ₃	IIIB	2300	11	20	1199.3	2.74	1.69	95.90	1.10	5.580	0.0126	0.135	31.10					hexagonal	28.54	16
58	CeO ₂	LANT	2397	26	26	1089.3	2.70	1.65	2500.00	1.12	5.540	0.0115	0.114	29.60					cubic	27.75	18
60	Nd ₂ O ₃	LANT	2315	12	28	1206.2	2.64	1.64	5930.00	1.14	5.530	0.0157	0.165	31.40						28.67	25
62	Sm ₂ O ₃	LANT	2320	19	23	1211.1	2.59	1.62	1860.00	1.17	5.640	0.0096	0.133	30.10	2.100	9.927		0.051		28.42	14
63	Eu ₂ O ₃	LANT	2330	16	27.5	1156.4	2.56	1.85	30900.00	1.20	5.670	0.0112	0.139	28.80	2.105	10.047		0.051	cubic	27.84	23
64	Gd ₂ O ₃	LANT	2395	12	26.5	1211.2	2.54	1.61	185000.00	1.20	6.150	0.0074	0.106	27.70	2.093	10.265		0.052	cubic	27.24	19
66	Dy ₂ O ₃	LANT	2385	18	36	1244.4	2.49	1.59	98000.00	1.22	5.940	0.0108	0.107	24.50	2.041	10.236		0.058	cubic	28.62	25
67	Ho ₂ O ₃	LANT	2395	37	40	1253.8	2.47	1.58	72900.00	1.23	6.018	0.0124	0.162	23.60	1.960			0.068	cubic	29.55	32.5
68	Er ₂ O ₃	LANT	2400	36	39.5	1265.3	2.45	1.57	48000.00	1.24	6.101	0.0117	0.143	22.70	1.950	27.611		0.069	cubic	26.43	28
69	Tm ₂ O ₃	LANT	2425	34	32	1259.4	2.42	1.56	24700.00	1.25	6.184	0.0150	0.168	21.80	1.950			0.069	cubic	27.35	28
70	Yb ₂ O ₃	LANT	2420	30	32	1210.0	2.40	1.74	67.00	1.10	6.254	0.0351	0.349	21.00	1.940	8.160		0.071	cubic	26.15	29
71	Lu ₂ O ₃	LANT	2467	29	35	1252.1	2.25	1.56		1.27	5.430	0.0185	0.164	21.90	1.930	7.962		0.072		27.81	26
72	HfO ₂	IVB	2790	30	30	1113.7	2.16	1.44	75.00	1.30	6.650	0.0312	0.230	16.20	2.000	4.164		0.063	monoclinic	25.79	18
77	IrO ₂	VIII	1100	24	30.5	184.2	1.87	1.27	25.60	2.20	9.100	0.1970	1.470	7.60					tetragonal	32.01	16
90	ThO ₂	ACTI	3300	22	30	1227.6		1.65	132.00	1.30	6.080	0.0653	0.540	32.10	2.200	5.870		0.043	cubic	26.51	14

**Fig. 7**

2025-04-10 10:00:00

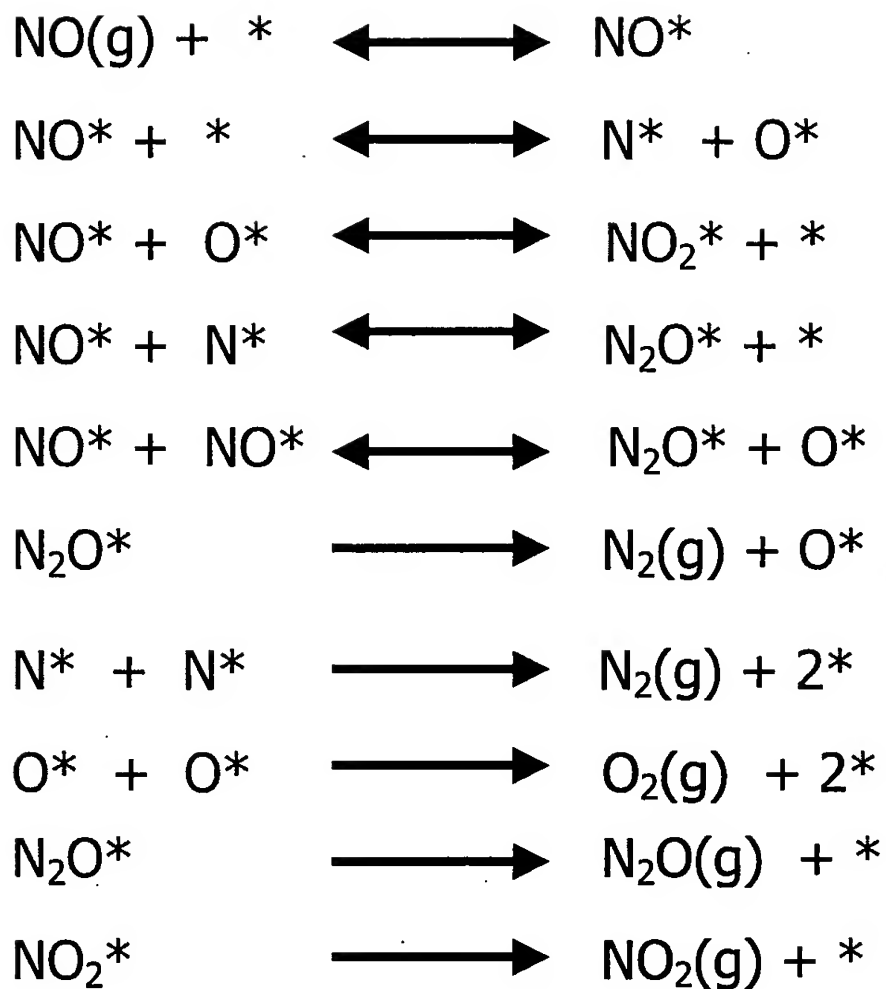


Fig. 8

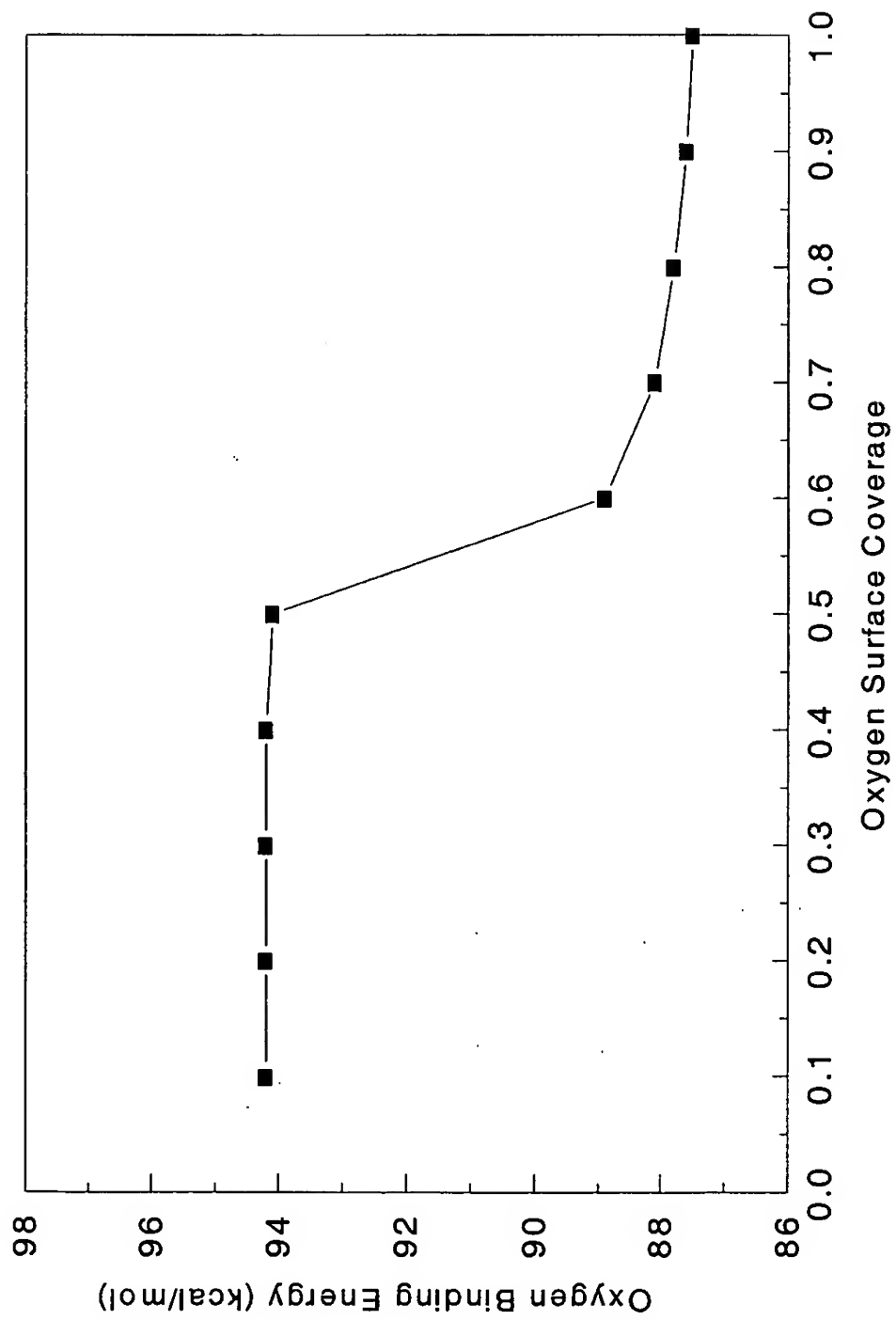


Fig. 10

20250320-44223001

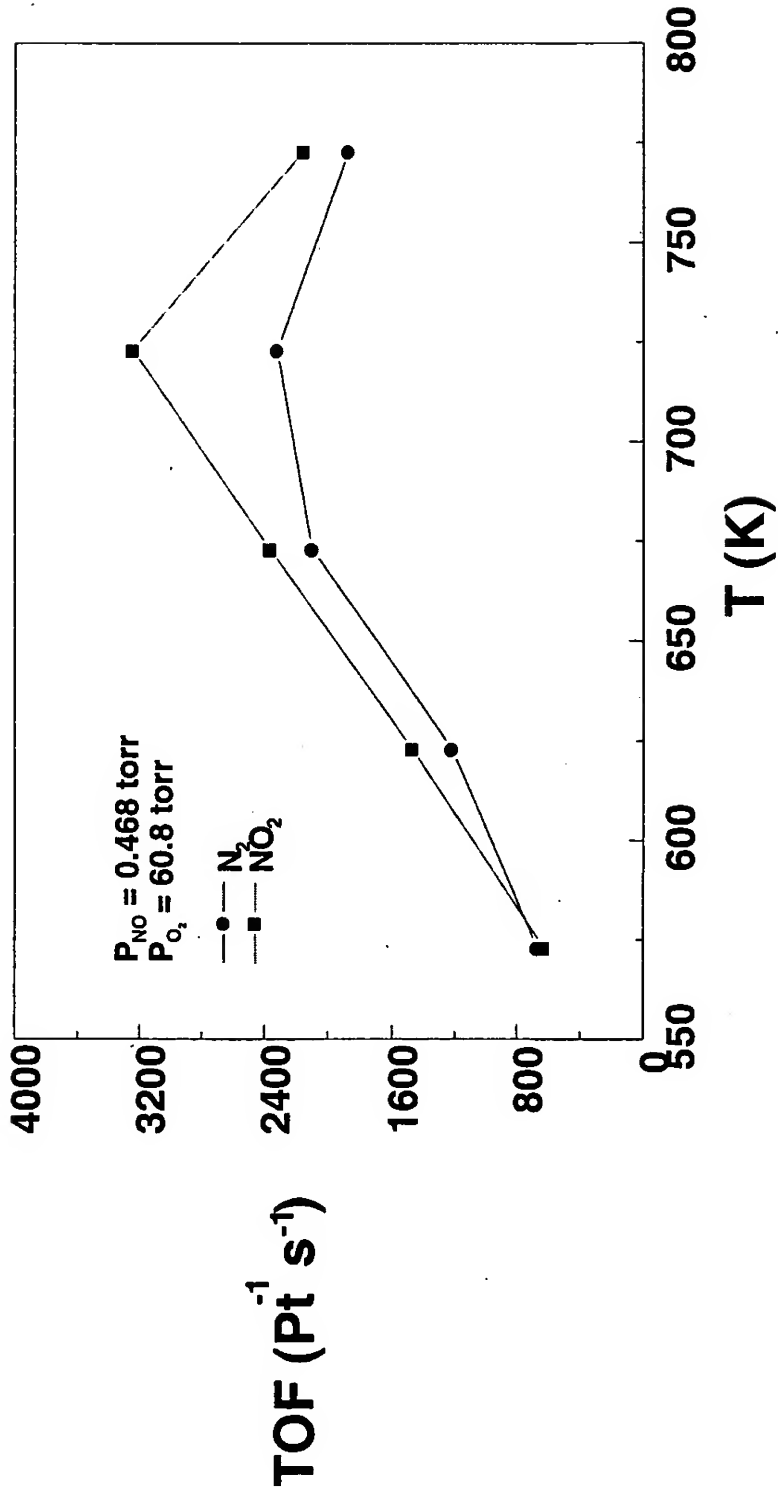


Fig. 11

ATTORNEY REF. NO. 122191-101C1

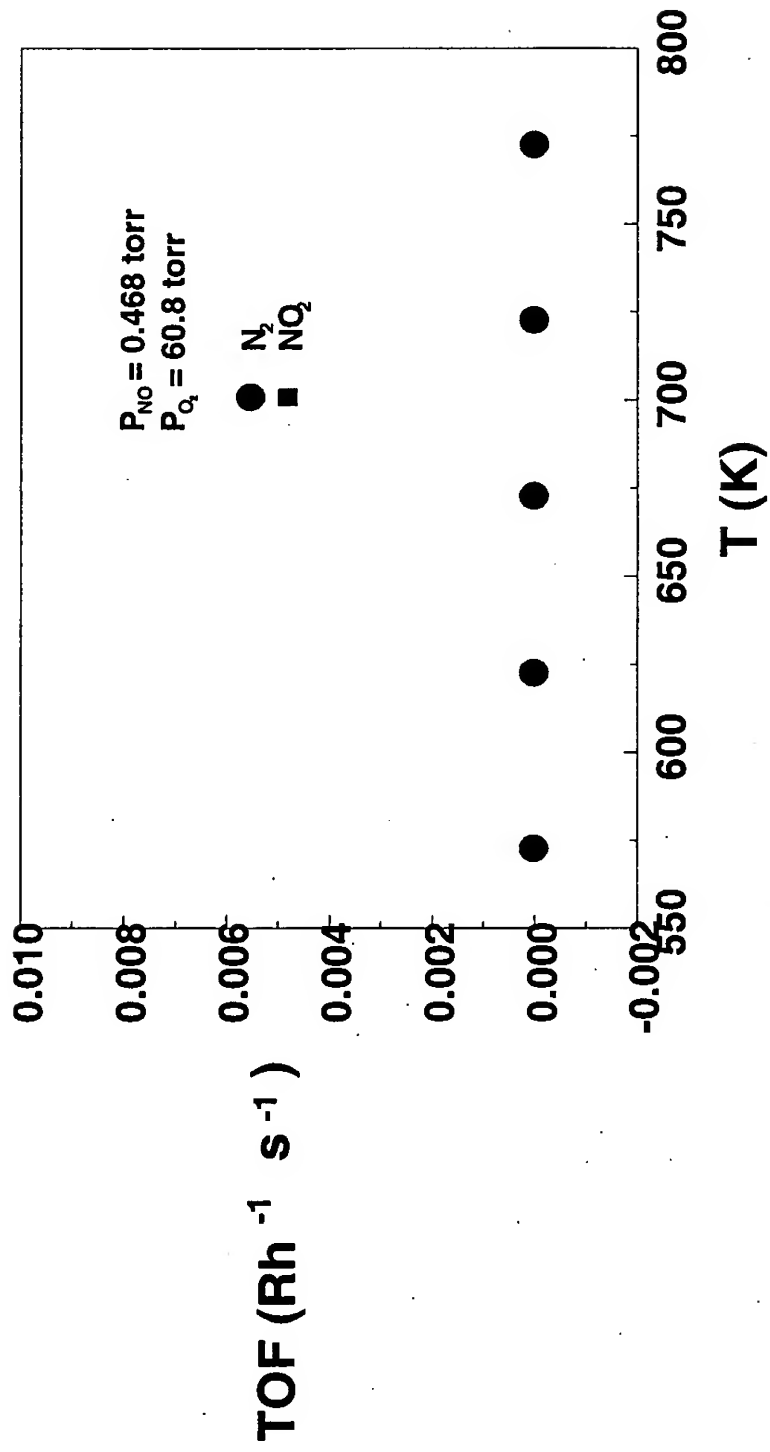


Fig. 12

205020 "4/23/2001"

Periodic Trends in Chemisorption and Activation Energies

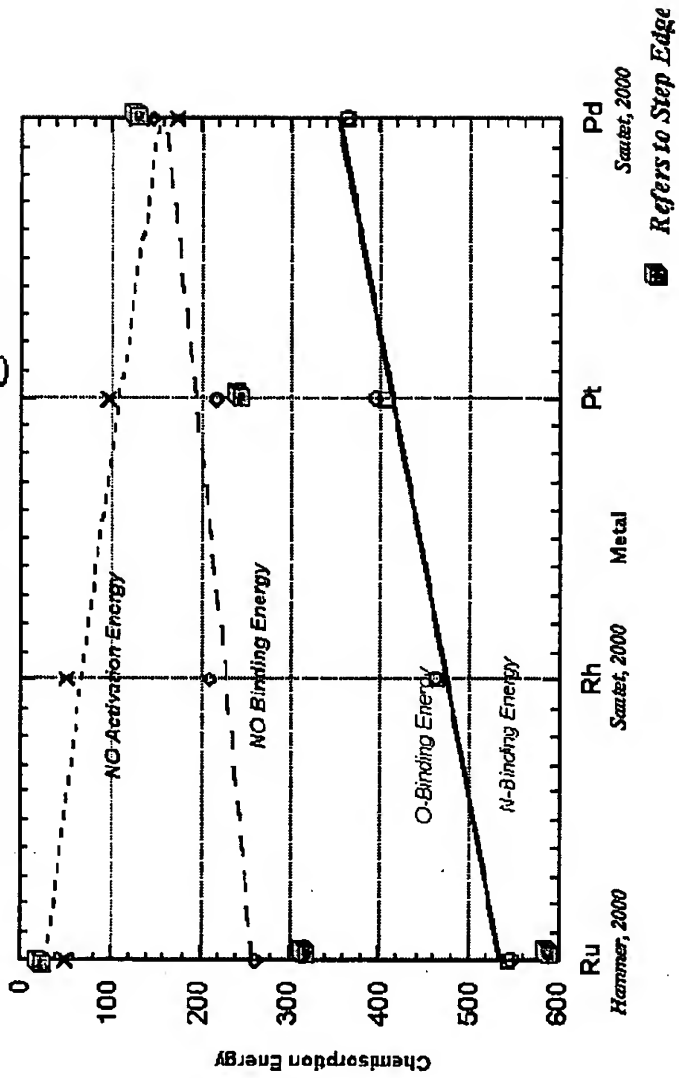


Fig. 13

Structure Sensitivity for NO Decomposition

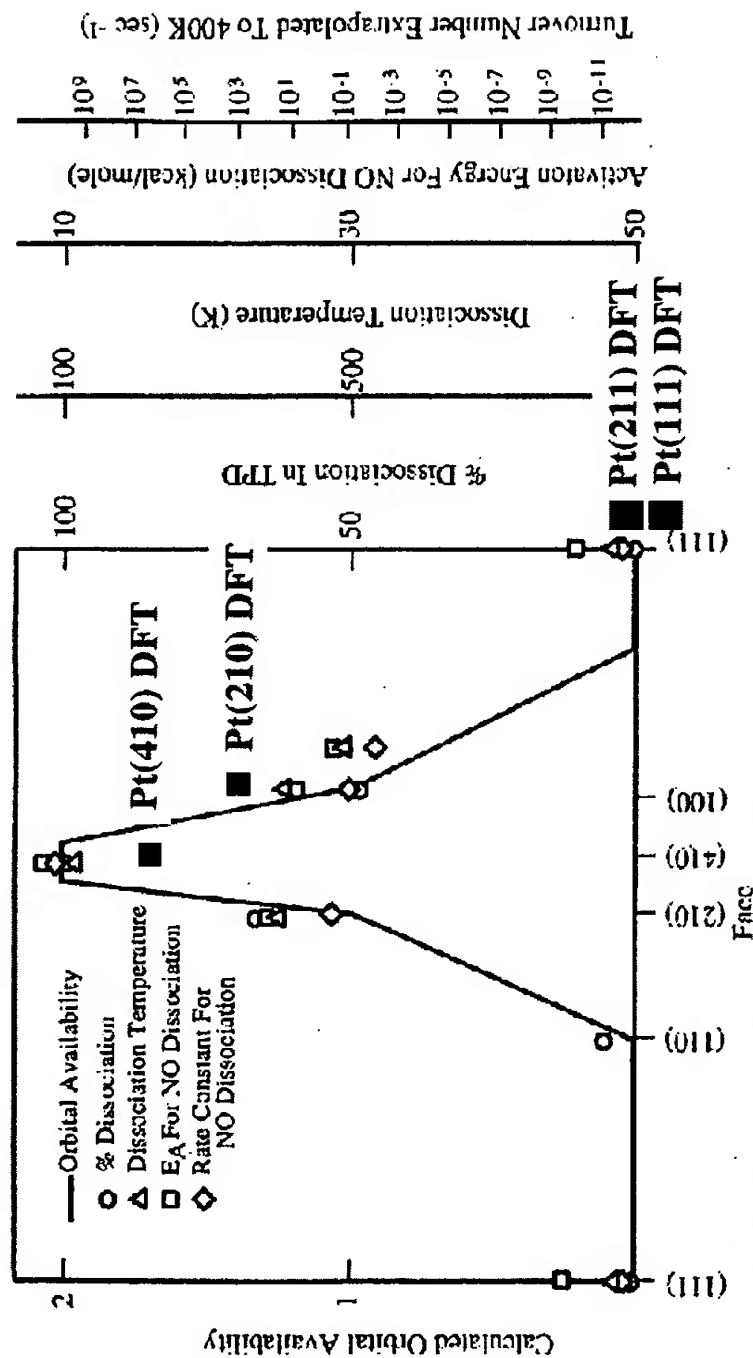


Figure 6.14 The rate on nitric oxide dissociation on several of the faces of platinum along the principle zone axes of the stereographic triangle. (Adapted from Masel [1983].)

Fig. 14

205020 44289001

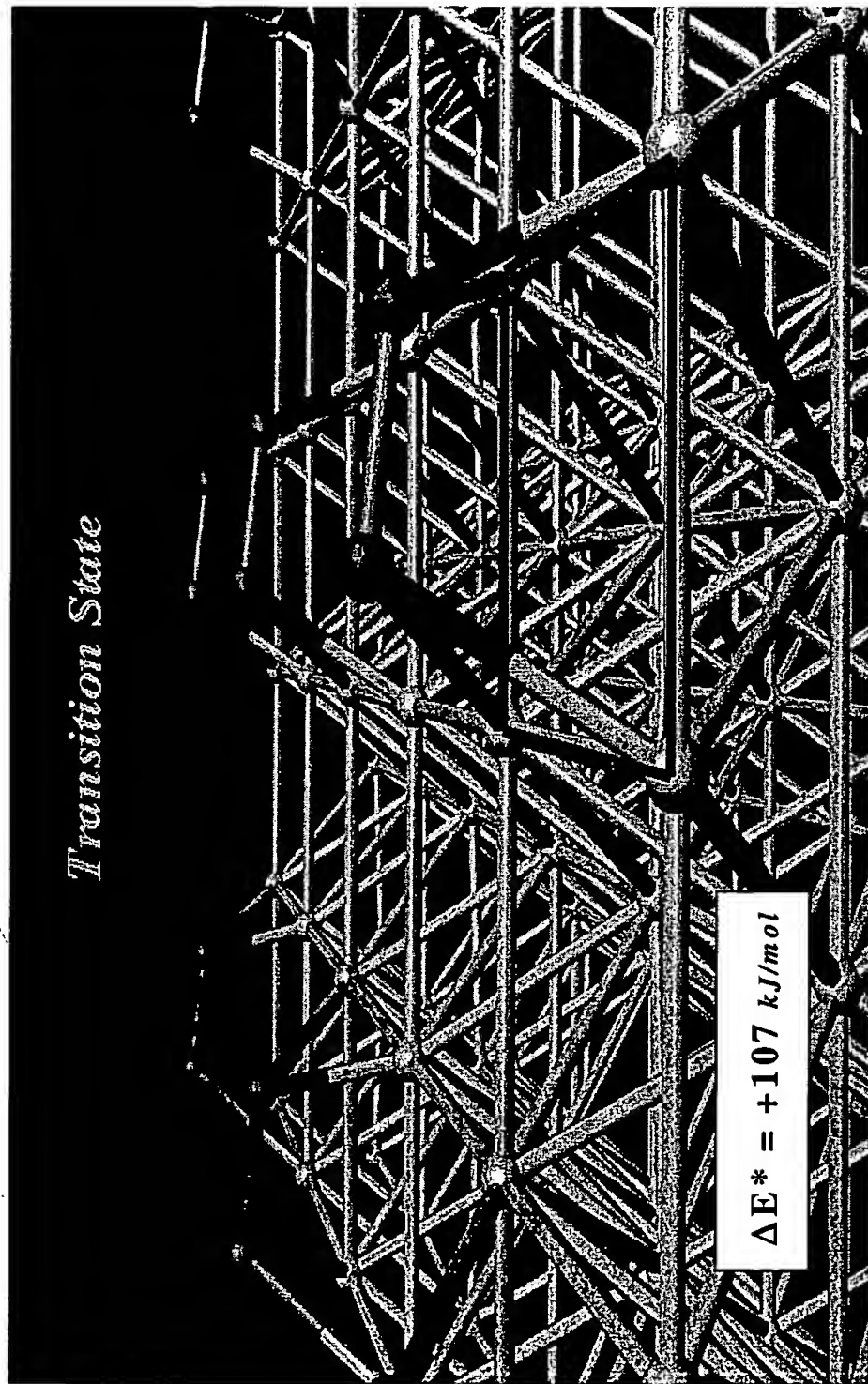
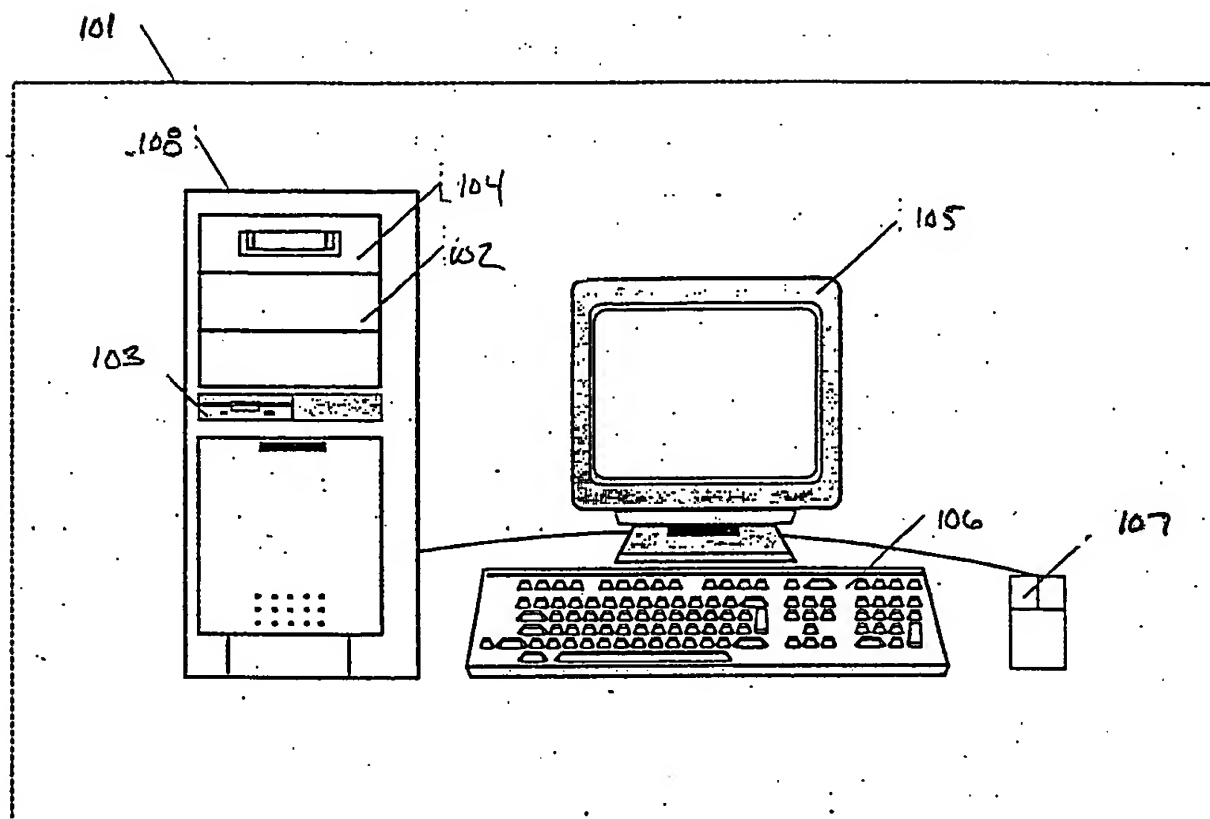


Fig. 15

FIG. 16 Representative Computer



10066244-000506

FIG 1 Computer System Internal Diagram

